THE JOURNAL OF BIOLOGICAL CHEMISTRY
Vol. 273, No. 8, Issue of February 20, pp. 4350–4359, 1998
Printed in U.S.A.

Structural Modification of Fibroblast Growth Factor-binding Heparan Sulfate at a Determinative Stage of Neural Development*

(Received for publication, August 27, 1997, and in revised form, December 1, 1997)

Yardenah G. Brickman‡, Miriam D. Ford, John T. Gallagher§, Victor Nurcombe, Perry F. Bartlett¶, and Jeremy E. Turnbull§‖

From the Department of Anatomy and Cell Biology, University of Melbourne, Victoria, Australia 3052, the ¶Walter and Eliza Hall Institute of Medical Research, Royal Melbourne Hospital, Victoria, Australia 3050, and the §CRC Medical Oncology Department, University of Manchester, Christie CRC Research Centre, Manchester, M20 4BX United Kingdom

Heparan sulfate (HS) glycosaminoglycans are essential modulators of fibroblast growth factor (FGF) activity and appear to act by coupling particular forms of FGF to appropriate FGF receptors. During neural development, one particular HS proteoglycan is able to rapidly switch its potentiating activity from FGF-2, as neural precursor cell proliferation occurs, to FGF-1, as neuronal differentiation occurs. Using various analytical techniques, including chemical and enzymatic cleavage, low pressure chromatography, and strong anion-exchange high performance liquid chromatography, we have analyzed the different HSs expressed during these crucial developmental stages. There are distinct alterations in patterns of 6-*O*-sulfation, total chain length, and the number of sulfated domains of the HS from the more mature embryonic brain. These changes correlate with a switch in the ability of the HS to potentiate the actions of FGF-1 in triggering cell differentiation. It thus appears that each HS pool is designed to function in the modulation of an intricate interaction with a specific growth factor and its cognate receptor, and suggests tightly regulated expression of specific, bioactive disaccharide sequences. The data can be used to construct a simple model of controlled variations in HS chain structure which have functional consequences at a crucial stage of neuronal maturation.

Heparin-binding fibroblast growth factors (FGFs)[1] are essential regulators of mitogenesis and differentiation for the precursor cells of the mammalian central nervous system (1). As in many tissues, the bioactivity of the FGFs is partially regulated by the glycosaminoglycan heparan sulfate (HS). These carbohydrate chains are normally found attached to core proteins and cells lacking these heparan sulfate proteoglycans (HSPGs) are unable to transduce an FGF signal (2, 3). One current hypothesis is that HSs serve to couple FGFs to specific HS-binding regions on competent FGF receptors (FGFRs) to form activating ternary complexes (4, 5). We have previously purified two different species of HSPG from embryonic murine neuroepithelia: from embryonic day 10 (E10) cells, when an HSPG with an affinity for FGF-2 was found and whose sugar chains are herein designated as HS2, and from E12 neuroepithelial cells, when an HSPG with an affinity for FGF-1 is expressed, and whose sugar chains are called HS1 (6, 7). This switch in HSPG activating activity was coincident with a similar switch in FGF expression. As the HSPG core protein carrying the two HS species appeared to be the same (6) then presumably differences in HS structure between E10 and E12 must account for the change in FGF specificity.

As specific HS species are essential to FGF activation, knowledge of the structures is clearly crucial to understanding their potentiating functions. Variation in HS species arises from the synthesis of non-random, highly sulfated sequences of sugar residues which are separated by unsulfated regions of disaccharides containing *N*-acetylated glucosamine. The initial conversion of *N*-acetylglucosamine to *N*-sulfoglucosamine creates a focus for other modifications, including epimerization of glucuronic acid to iduronic acid and a complex pattern of *O*-sulfations on glucosamine or iduronic acids (8, 9). In addition, within the non-modified, low sulfated, *N*-acetylated sequences, the hexuronate residues remain as glucuronate, whereas in the highly sulfated *N*-sulfated regions, the C-5 epimer iduronate predominates (10–12). This limits the number of potential disaccharide variants possible in any given chain but not the abundance of each. Most modifications occur in the *N*-sulfated domains, or directly adjacent to them, so that in the mature chain there are regions of high sulfation separated by domains of low sulfation (12–15). This pattern distinguishes HS from heparin, which is essentially highly sulfated along its entire length. Some of these modifications have been shown to be essential in creating unique binding sites for molecules such as antithrombin III, FGF-2, hepatocyte growth factor, and interferon-γ (16–21). The possibility therefore exists that such modifications may create specific binding sites for different members of the FGF family and many other extracellular matrix molecules.

This study presents a detailed structural comparison of two HS preparations: HS1 from E12 primary murine neuroepithelia and HS2 from E10 primary murine neuroepithelia. (22). It has now been well established that cells are capable of changing both the glycosaminoglycan moiety attached to a specific core protein, and the sulfation patterns of HSs in culture (23–

* This work was supported in part by the National Health and Medical Research Council of Australia and the United Kingdom Cancer Research Campaign. The costs of publication of this article were defrayed in part by the payment of page charges. This article must therefore be hereby marked "*advertisement*" in accordance with 18 U.S.C. Section 1734 solely to indicate this fact.

‡ Supported by an Overseas Postgraduate Research Award and a Melbourne University Postgraduate Scholarship. To whom correspondence should be addressed: Van Cleef/Roet Centre for Nervous Diseases, Dept. of Medicine (Dept. of Neuroscience), Monash University, Alfred Hospital, Commercial Rd, Prahran. Victoria 3181, Australia. E-mail: Yardenah.Brickman@med.monash.edu.au; Tel.: 03-9276-2697; Fax: 9276-2458.

‖ Present address: School of Biochemistry, University of Birmingham, Edgbaston, Birmingham, B15 2TT, United Kingdom. E-mail: j.e.turnbull@bham.ac.uk.

[1] The abbreviations used are: FGF, fibroblast growth factor; HS, heparan sulfate; HSPGs, heparan sulfate proteoglycans; E10, embryonic day 10; SAX-HPLC, strong anion exchange-high pressure liquid chromatography; GlcA, glucuronic acid; $AMan_R$, reduced anhydromannose; IdoA, iduronic acid; GlcNAc, *N*-acetylated glucosamine; $GlcNSO_3$, *N*-sulfated glucosamine; HexA, hexuronic acid.

27), just as they do over the course of development, injury, and disease (23, 28, 29). The main aim of this study was to elucidate the structures of the two HS species which mediate either mitogenesis or differentiation *in vivo*, and to determine the structural properties that may account for the selectivity for the two FGFs. Although direct sequencing of whole HS chains is not yet feasible, methods for identifying specific structural elements within a pool of similar chains are available. The conjoint use of heparin lyases and nitrous acid digestion, low pressure chromatography, HPLC, and a unique tetrasaccharide analysis have allowed us to elucidate subtle structural and compositional differences between mixtures. The results of the structural analysis have led to the construction of a model for the changing HS pools.

EXPERIMENTAL PROCEDURES

Materials—Trypsin was supplied by Calbiochem and DNase from Boehringer Mannheim. D-[6-^{3}H]Glucosamine (specific activity 21 Ci/mmol) was obtained from Amersham Life Science. Heparitinases I (EC 4.2.2.8), II (no EC number assigned), and III (EC 4.2.2.7) and chondroitin ABC lyase (EC 4.2.2.4) were obtained from Seikagaku Kogyo Co., Tokyo, Japan. Heparitinase IV was from Sigma (Sydney, Australia). Cell culture media was supplied by Life Technologies, Inc. Bio-Gel P-2 and P-10 were from Bio-Rad Laboratories. CL-6B gel, DEAE-Sephacel, columns, peristaltic pumps, fraction collectors, and tubing were from Pharmacia Biotech Inc. (Sydney, Australia). ProPac PA1 analytical columns for the HPLC were from Dionex (Surrey, United Kingdom). Centriflo CF25 Membrane Cones were supplied by Amicon (Sydney, Australia). Scintillant (Ultima Gold) was from Packard (Melbourne, Australia) as were the scintillation vials. All chromatographic procedures were carried out a minimum of 3 times, and the standard errors on all peaks reported in this study were never more than 8%.

Cell Culture and Labeling—Primary neuroepithelial cells were grown in 10% FCS/Dulbecco's modified Eagle's medium and 2 ng/ml FGF-2 in 24-well tissue culture plates at a density of 100,000 cells/well for E10, and 200,000 cells/well for E12. Post-plating (30–60 min), 20 μCi/ml [^{3}H]glucosamine was added. Cultures were further incubated for 3–4 days, with the E12 cells being at confluence. HS from these preparations was designated HS2 and HS1 for E10- and E12-derived HS, respectively. The conditioned medium was removed and centrifuged (1000 rpm for 5 min) to remove any cell debris and stored at −20 °C until required.

Preparation of Intact Heparan Sulfate Chains—The conditioned media was subjected to ion-exchange chromatography on a DEAE-Sephacel column (3 ml) equilibrated in 150 mM NaCl with phosphate-buffered saline, pH 7.2. The media was manually loaded onto the column and eluted under gravity. The column was washed with 10 column volumes of 250 mM NaCl in 50 mM phosphate-buffered saline, pH 7.2. The bound material was eluted with 1 M NaCl in 50 mM phosphate-buffered saline and 2-ml fractions collected. Fractions containing the [^{3}H]glucosamine-labeled glycosaminoglycans were pooled, concentrated, and desalted on Centriflo Cones (as per manufacturer's instructions), freeze dried, and resuspended in a minimal volume (100–500 μl) of neuraminidase buffer (25 mM sodium acetate, pH 5.0). Samples were treated with neuraminidase (0.25 unit/sample) for 4 h. Five volumes of 100 mM Tris acetate, pH 8.0, were then added to the sample which was then digested with chondroitin ABC lyase (0.25 unit/sample) for 4 h at 37 °C and further digested overnight with an equal amount of fresh enzyme. Finally, the core protein and the lyases were digested away with Pronase (1/5 total volume of 10 mg/ml Pronase in 500 mM Tris acetate, 50 mM calcium acetate, pH 8.0) at 37 °C for 24 h. The entire mixture was then diluted 1:10 with deionized water, passed through a 2-ml DEAE-Sephacel column, eluted as described previously, and 1-ml fractions collected. The sample was finally desalted on a 1 × 35-cm Bio-Gel P-2 column, the V_o fraction collected and freeze dried.

Heparan Sulfate Characterization—To remove HS chains from trace amounts of core protein, samples were incubated in 500 mM NaOH, 1 M $NaBH_4$ for 16 h at 4 °C and neutralized to pH 7 with glacial acetic acid. Concentrated ammonium bicarbonate was added and after the bubbling stopped, samples were run on a CL-6B column (1 × 120 cm) for sizing of the released HS chains (30). Binding experiments were performed on these HS preparations as described under "Results."

Nitrous Acid Treatment of HS Chains—HS was chemically depolymerized by low pH HNO_2 (pH <1.5) as described by Shively and Conrad (31) and modified by Bienkowski and Conrad (32). Linkages susceptible to low pH HNO_2 are those containing *N*-sulfates of the type $GlcNSO_3(\pm 6S)\alpha 1\text{–}4UA(\pm 2S)$ (11), whereas the resistant linkages are UA $\alpha 1\text{–}4$ $(GlcNAc(\pm 6S)\alpha 1\text{–}4GlcA)_n\text{-}GlcNSO_3$. A small portion of the mixture was run on a Bio-Gel P-10 column (1 × 200 cm) to obtain a profile of the fragments released by this treatment and the rest of the mixture was separated on a Bio-Gel P-2 column (1 × 120 cm) to isolate disaccharides and tetrasaccharides for strong anion exchange-high pressure liquid chromatography (SAX-HPLC).

Lyase Depolymerization of HSPGs—Heparitinase (heparitinase I), heparitinase II, and heparitinase IV were used at a concentration of 25 milliunits/ml in 100 mM sodium acetate, 0.2 mM calcium acetate, pH 7.0. Heparinase was used at a concentration of 50 milliunits/ml in the same buffer. Heparitinase I (also known as heparinase III) cleaves mainly at $GlcNR(\pm 6S)\alpha 1\text{–}4$ GlcA linkages (R = *N*-acetyl or *N*-sulfate moiety) (11, 33) creating resistant products with the structural motif GlcA $\alpha 1\text{–}4(GlcNSO_3(\pm 6S)\alpha 1\text{–}4IdoA(+2S))_n$ $\alpha 1\text{–}4$ GlcNR. Heparitinase II (also known as heparinase II) has a wide spectrum of activity cleaving linkages of the type $GlcNSO_3(\pm 6S)\alpha 1\text{–}4IdoA/Glc$ leading primarily to the generation of disaccharides from HS (33). Heparinase (also known as heparitinase III) cleaves at linkages of the type $GlcNSO_3(\pm 6)\alpha 1\text{–}4IdoA(2S)$ (11, 33) creating resistant sequences of structure $IdoA(2S)\alpha 1\text{–}4(GlcNR(\pm 6S)\alpha 1\text{–}4UA)\beta 1\text{–}4GlcNSO_3(\pm 6S)$ (R = *N*-acetyl or *N*-sulfate moiety) (11, 33). Samples were digested in the presence of 100 μg of non-labeled carrier HS. For single enzyme digests, samples were separately incubated at 37 °C for 16 h and then a second aliquot of enzyme added and incubated for a further 4 h. Sequential digests for recovery of disaccharides for SAX-HPLC analysis were performed in the presence of 100 μg of nonlabeled HS at 37 °C as follows: heparinase for 2 h, heparitinase for 1 h, heparitinase II for 18 h, and finally an aliquot of each lyase and heparitinase IV for 6 h. Sample volumes were decreased to less than 100 μl by desiccation and run on a Bio-Gel P-2 column to isolate disaccharides.

Gel Chromatography—Gel chromatography of intact chains or scission products was performed on Sepharose CL-6B (1 × 120 cm) or Bio-Gel P-2 (1 × 120 cm) or Bio-Gel P-10 (1 × 200 cm) columns. The running buffer for the CL-6B and Bio-Gel P-10 columns was 0.5 M NH_4HCO_3 and for the Bio-Gel P-2 column was 0.25 M NH_4HCO_3. Samples were routinely eluted at 4 ml/h with 1-ml fractions collected. For preparative runs, the radioactivity of a small aliquot of each fraction (1–10 μl) was monitored by liquid scintillation counting to ensure good separation and accurate isolation of fragments for further analysis. Estimates of the size of fragments resolved on Sepharose CL-6B were based on published calibrations (30).

SAX-HPLC Analysis of Disaccharides and Tetrasaccharides—Disaccharide composition of the HS was analyzed on SAX-HPLC after either complete depolymerization with a mixture of lyases as described above or HNO_2 treatment. Disaccharides and/or tetrasaccharides were recovered by Bio-Gel P-2 chromatography and fractions corresponding to disaccharides or tetrasaccharides were pooled, freeze dried, and stored at −20 °C. The lyase-derived disaccharides were subjected to SAX-HPLC on a ProPac PA1 analytical column (4 × 250-mm Dionex Ltd.) as follows. After equilibration in the mobile phase (double-distilled water adjusted to pH 3.5 with HCl) at 1 ml/min, samples were injected and disaccharides eluted with a linear gradient of NaCl from 0 to 1 M over 45 min in the same mobile phase. The eluant was collected in 0.5-ml fractions and monitored for tritium-labeled disaccharide content for comparison with lyase-derived disaccharides standards. Nitrous acid-derived tetrasaccharides were subjected to the same conditions (with 0.25- or 0.5-ml fractions collected) and compared with double labeled standard results which were supplied by Dr. Gordon Jayson (Christie Hospital, Manchester, UK). Alternatively, HNO_2-derived disaccharides were separated using two ProPac PA1 columns in series in the same mobile phase. A shallow, non-continuous gradient was used over the course of 97 min. After a 1-min injection phase, a 50-min gradient from 0 to 150 mM NaCl was employed, followed by a 70-min gradient of 150–500 mM NaCl. The eluant was collected as described above and compared with standards. Major peaks are labeled in Fig. 3*A* and three minor disaccharide peaks eluted as follows: $GlcA(2S)\text{-}AMan_R$ between 43.75 and 44 min, $GlcA\text{-}AMan_R(3S)$ between 45.75 and 46.5 min, and $GlcA\text{-}AMan_R(3,6S)$ between 104 and 106 min.

Nitrocellulose Filter Binding Assays—Nitrocellulose filter binding assays were performed as described previously (34) with modifications. Briefly, ^{3}H-labeled HS samples were incubated with 5 μg of the appropriate FGF for 10 min at 37 °C in 0.5 ml of 10 mM Tris-HCl buffer, pH 7.0, and the complex immobilized by vacuum filtration onto a 25-mm diameter nitrocellulose filter. The HS was then step eluted by consecutively vacuum filtering a series of 10 mM Tris-HCl, pH 7.0, solutions (5 ml each) containing increasing concentrations of NaCl (250, 500, 750,

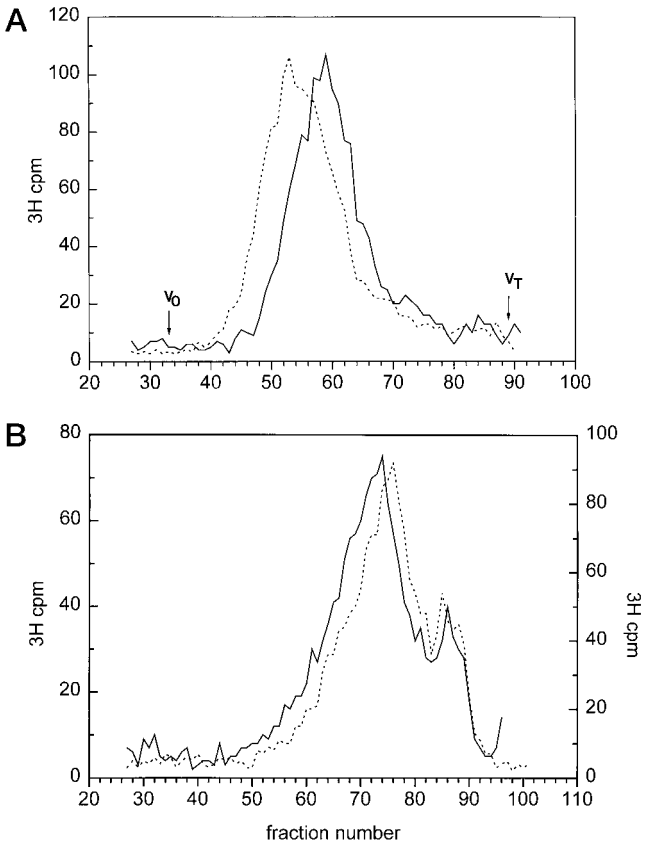

FIG. 1. **Gel filtration on Sepharose CL-6B of HS chains and fragments.** Heparan sulfate from primary neuroepithelial cells (*A* and *B*) was isolated and the size of the full-length chains (*A*) and heparinase-resistant fragments (*B*) determined using a Sepharose CL-6B gel filtration column (HS2, —; HS1, - - -). The results are summarized in Table I.

1000, 1250, 1500, and 2000 mM) through the nitrocellulose membrane. Radioactivity in the filtrate at each NaCl concentration was measured by scintillation counting.

RESULTS

The structural features of the HS chains were investigated using established protocols (12, 35–37). HS chains (derived by Pronase and mild alkali treatment) were chromatographed on Sepharose CL-6B columns either intact, or after heparinase treatment (Fig. 1 and Table I). Both pools of HSPGs showed a partial resistance to proteolysis by Pronase, characteristic of proteoglycans, which are densely substituted with polysaccharide chains. This data indicates that there are at least two HS chains per core protein in each preparation, and that their attachment sites are located close together. HS^2 and HS1 eluted at K_{av} of 0.46 and 0.36, respectively, which corresponds to average molecular masses of 25 and 40 kDa when compared with published calibrations (30). Assuming an average molecular mass of 400 Da per disaccharide, HS2 and HS1 are 60 and 100 disaccharides in length, respectively. The HS expressed early in development is thus smaller than the more mature chains, indicating significant structural changes underlying the functional differences exhibited in previous studies.

Low pH HNO_2 Treatment—To determine the number and general organization of *N*-sulfated disaccharides the HS samples were subjected to low pH HNO_2 treatment. Low pH scission releases the *N*-sulfate groups from heparan sulfate with subsequent cleavage of the adjacent hexosaminidic bond. This gave elution profiles (Fig. 2*A*) with a typical distribution of *N*-sulfated disaccharides characteristic of HS (38). From these profiles it is possible to calculate the percentage of linkages

TABLE I
A summary of the estimated M_r of extracellular-HS from the two samples examined in this study

All HS samples were subjected to separation on a 1 × 120-cm Sepharose CL-6B column after a variety of treatments. The size of purified full-length HS was determined both before and after mild alkali treatment to determine the presence of more than one chain per protein core. In addition, the approximate distance between heparinase-sensitive disaccharides was determined by isolating the non-resolved, large oligosaccharides from a Bio-Gel P-10 column (Fig. 2*B*, V_o peak) and rerunning them on a Sepharose CL-6B column.

Condition	HS2	HS1
Pronase (Da)	40,000	70,000
Mild alkaline (Da)	25,000	40,000
Heparinase (Da)	7,000	5,000
No. heparinase-resist domains	2	7–8

susceptible to this treatment and thus the percentage of *N*-sulfated glucosamine residues in the HS chains. HS2 was significantly more susceptible to nitrous acid cleavage than HS1 (Table II). As the similarities between the profiles confirm, the results also show the strong tendency of the *N*-sulfated disaccharides to occur in contiguous or mixed sequences. There is a small decrease in the proportion of repeating *N*-acetylated disaccharide sequences in HS1 that might be due to a reduction in the spacing between the sulfated domains.

Chromatography of Lyase-treated HS—Heparinase-treated oligosaccharides were separated on a Bio-Gel P-10 column (Fig. 2*B*). The molecular mass of the heparinase-resistant domains in HS corresponds to the average distance between the centers of highly sulfated regions which contain heparinase-susceptible linkages. Analysis of the percentage of small oligosaccharides (degree of polymerization 2–6) (*inset* Fig. 2*B*) released by this treatment revealed that HS2 released approximately 50% fewer small oligosaccharides then HS1. Estimation of the molecular size of the material excluded from the P-10 column by CL-6B chromatography (Fig. 1*B*) showed that the major peaks correspond to molecular weights of 7,000 and 5,000 (Table I), respectively, for HS2 and HS1, although there is considerable overlap of the two peaks, indicating a broad similarity in size distribution. The results do suggest a tendency for closer average positioning of the sulfated domains in the more mature E12 chains, although more work will have to be done to confirm this point. Heparinase therefore cuts the HS2 chains into 3–4 segments but in contrast cuts the HS1 chains into 7–8 segments. HS2 is therefore less complex in domain structure than HS1. Heparitinase treatment of the samples yielded elution profiles (Fig. 2*C*) which were also characteristic of HS (12). The heparitinase cleavage also tends to confirm that the sulfated domains are broadly similar in size from E10 to E12, the only significant difference being a decrease in the tetrasaccharide peak in HS1. Quantitative analysis of the profiles demonstrated that 61 and 65% of the linkages in HS2 and HS1 were susceptible to this treatment, respectively (*i.e.* GlcA-containing disaccharides), a result which indicates that the sizes of the (heparitinase-resistant) sulfated domains in both E10 and E12 material are broadly similar. The remaining disaccharides must contain IdoA or IdoA(2S), indicating that there is a slightly higher content of IdoA(±2S) residues in HS2 chains. Since HS2 is less susceptible to heparinase (Table II), which cleaves at IdoA(2S) residues, and contains less 2-*O*-sulfated disaccharides (see Tables III and IV) this indicates that it contains a higher level of unsulfated iduronate than HS1.

SAX-HPLC of Nitrous Acid-generated Disaccharides—Oligosaccharides derived by HNO_2 treatment of HS were reduced with sodium borohydride, separated on a Bio-Gel P-2 column, pooled, and freeze dried. SAX-HPLC separation of disaccharides resulted in the elution profiles in Fig. 3. Nitrous acid

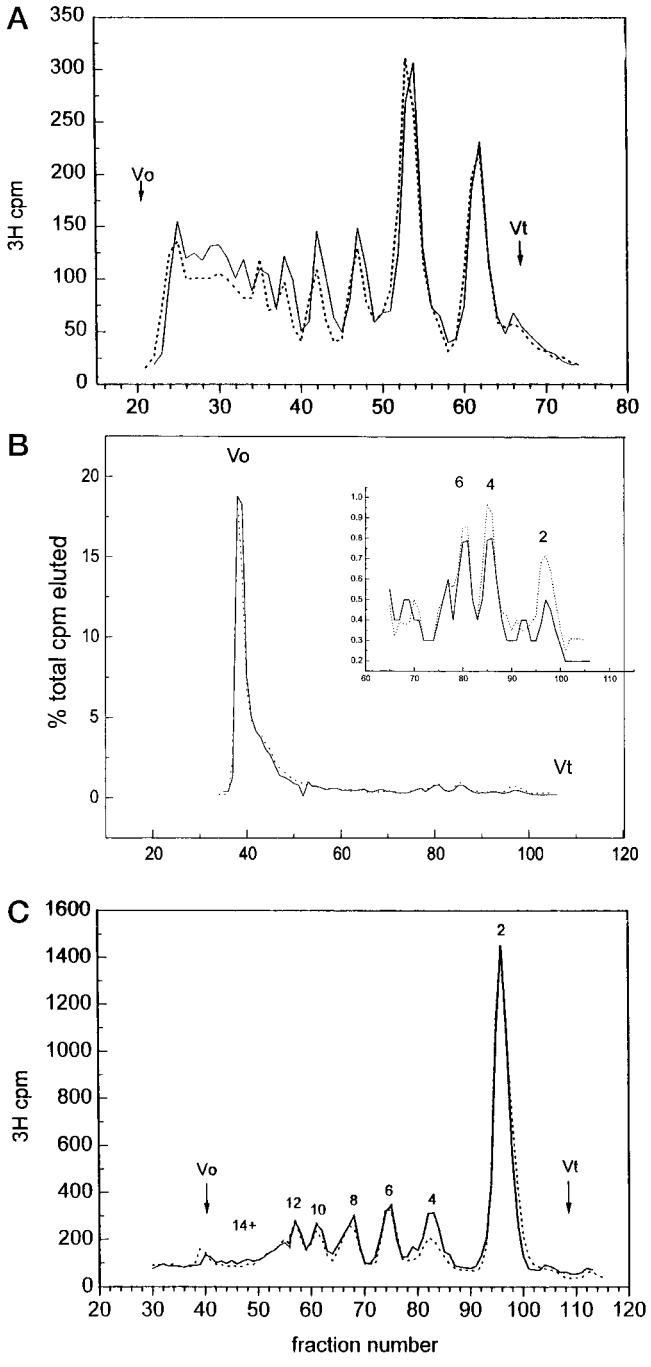

FIG. 2. **Gel filtration on Bio-Gel P-10 of oligosaccharides produced by various depolymerizing agents.** HS from primary neuroepithelial cells (*A-C*) was isolated as described in the text and was fractionated on a Bio-Gel P-10 column (1 × 200 cm) after the following treatments. *A*, low pH HNO_2 depolymerization. A small aliquot was fractionated on a Bio-Gel P-10 column and the rest of this digested sample was run on a Bio-Gel P-2 column (1 × 120 cm) to isolate the tetrasaccharides and disaccharides for SAX-HPLC analysis. This profile was used to calculate the percentage of HNO_2 susceptible linkages (Table II). A large fraction of this digest sample was run on a Bio-Gel P-2 column (1 × 120 cm) to isolate the tetrasaccharides and disaccharides for SAX-HPLC analysis. *C*, depolymerization by heparitinase: the susceptibility of each species to heparitinase was calculated from this profile and tabulated in Table II. The degree of polymerization of each peak is represented by the *number above* that *peak* and was subsequently used in the calculations. *B*, depolymerization by heparinase: *inset*, fractions 64–115 of the heparinase scission profile with an expanded scale to reveal the proportions of low M_r products. The nonresolved V_o peak was pooled, freeze dried, and resolved on a Sepharose CL-6B (Fig. 1).

TABLE II

Proportion of the linkages susceptible to low pH HNO_2, heparitinase and heparinase in HS2 and HS1

Radiolabeled heparan sulfate from the two different sources was treated with low pH HNO_2, heparinase, or heparitinase and fractioned on a Bio-Gel P-10 column as described in the text. The percentage of the total treatment-sensitive linkages was determined in two separate experiments by $\Sigma A_n/n$, where A_n is the percentage of total radioactivity in that peak, and n is the number of disaccharide repeat units in the oligosaccharides as determined by the elution position.

Treatment	HS2	HS1
	%	
Heparitinase	61.5	65
Heparinase	15.3	16.7
HNO_2	49.0	53.0

cleaves hexosaminidic bonds in HS leading to the production of saccharides with an authentic nonreducing end uronic acid, but the loss of N_2 from the reducing end glucosamine and its conversion to a 2,5-anhydromannose residue. For SAX-HPLC, this moiety was reduced to 2,5-anhydromannitol. Each disaccharide peak was identified according to its elution time in comparison with standard HNO_2-derived disaccharides. These results are summarized in Table III where the area under each peak has been integrated and shown as a percentage of total disaccharides released by HNO_2 digestion. The major differences are a decrease in IdoA(2S)-$AMan_R$ and increases in both IdoA(2S)-$AMan_R$(6S) and GlcA(2S)-$AMan_R$ accompanying the transition from E10 to E12. Overall, there is a slight increase in total sulfation in the contiguous *N*-sulfated domains of HS1 when compared with HS2. HS2 is therefore less sulfated than its more mature counterpart HS1.

Analysis of the Total Disaccharide Composition of the HS Pools—To fully characterize the composition of the samples of HS, the chains were subjected to complete lyase depolymerization using heparitinases I, II, III, and IV. The products of this digestion were separated on a Bio-Gel P-2 column with over 95% of the radioactivity accounted for in the disaccharide peaks (data not shown), indicating sufficiently complete digestion to provide a representative compositional analysis. For analysis on SAX-HPLC, the disaccharides were pooled and freeze dried. The peaks in Fig. 4 were identified by reference to authentic standards (38, 39). Overall, the disaccharide compositions of the HS samples were broadly similar (Table IV). However, there were significant increases in the trisulfated disaccharide ΔHexUA(2S)-$GlcNSO_3$(6S) and in the disaccharide ΔHexUA-(2S)-GlcNAc in the E12-derived HS1. Based on this data, comparisons of the sulfation characteristics can be made (Table V). *N*-Sulfation was identical, whereas *O*-sulfation was slightly higher in HS1 relative to HS2, due mainly to a higher level of 2-*O*-sulfation, with only a small increase in 6-*O*-sulfation apparent.

SAX-HPLC of Nitrous Acid-generated Tetrasaccharides—The tetrasaccharide products isolated after an HNO_2 depolymerization were separated by SAX-HPLC (Fig. 5). The general structure of tetrasaccharides is HexA-GlcNac-Glc-AHM, and *O*-sulfation can occur at C-6 of the amino sugars, C-2 of the nonreducing terminal uronic acid, and at C-3 of $GlcNSO_3$. Current knowledge of HS biosynthesis and structure indicates that HNO_2-resistant tetrasaccharides are likely to flank the contiguous *N*-sulfated domains (12, 20). The positions of non-, mono-, and disulfated peaks were established by comparison with dual $^{35}S/^{3}H$-labeled samples run under identical conditions. The percentage of each of the designated peaks as compared with the total population is summarized in Table VI. The level of the nonsulfated peak (UAα1–4GlcNAcβ1–4GlcAα1–4$AMan_R$ tetrasaccharides) was similar in the HS from E10 and E12. However, the proportions of nearly all of the monosulfated

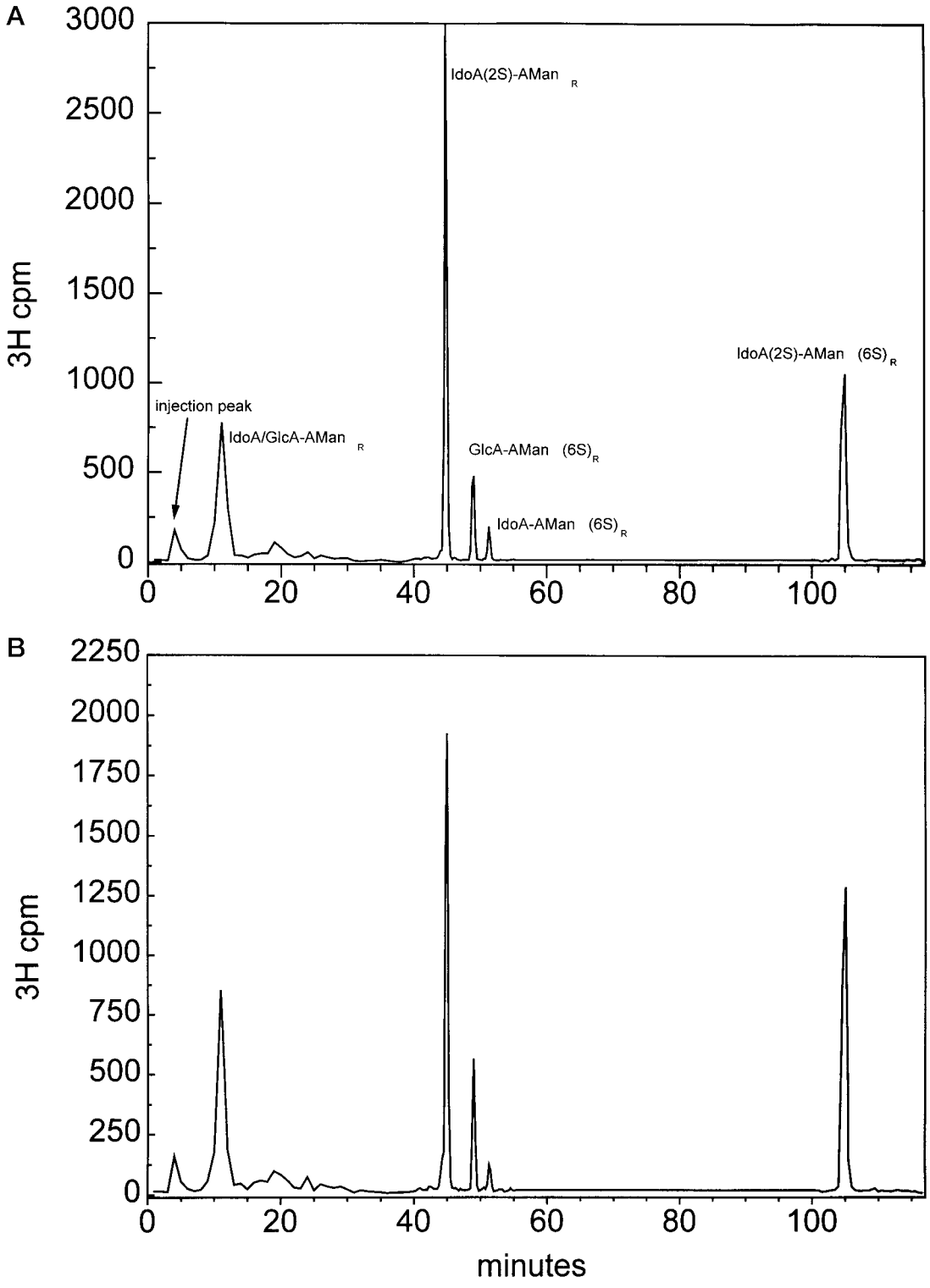

FIG. 3. **Strong anion exchange-high pressure liquid chromatography of HNO_2-generated disaccharides.** Disaccharides produced by low pH HNO_2 were isolated by Bio-Gel P-2 low pressure chromatography, freeze dried, and separated by SAX-HPLC. Disaccharides were eluted as described under "Experimental Procedures." The elution times of the peaks were compared with those of authentic standards and labeled accordingly. A representative elution profile from HS2 disaccharides is shown in *A* and HS1 disaccharides in *B*. The relative amounts of each of the peaks has been calculated and summarized for both HS pools in Table III.

peaks changed significantly, especially peaks 1 and 7, which decreased by 60 and 29%, respectively, and peak 5 which increased by 125%. The disulfated and trisulfated peaks also show small but significant changes in levels, and overall there is a slight trend toward increased sulfation at E12 in these tetrasaccharides. Thus, the tetrasaccharide analysis approach revealed considerable structural differences between the two HS pools, confirming the increased complexity in sulfation patterns during development.

Binding Assays—To confirm that the isolated heparan sulfate chains retain their binding specificities for particular FGFs, filter binding assays were performed. FGF-2 or FGF-1 were pre-mixed with either HS2 or HS1, and the complexes formed captured on a nitrocellulose filter and step eluted with

increasing concentrations of NaCl (Fig. 6). The results showed that the E10-derived HS pool, HS2, binds FGF-2 strongly and with a markedly greater affinity than for FGF-1. The E12-derived HS pool, HS1, also binds FGF-2, albeit a little more weakly than HS2 and would also appear to have, relative to HS2, an enhanced affinity for FGF-1.

TABLE III

Nitrous acid-derived disaccharide composition of heparan sulfate from HS preparations from two developmental stages of neuroepithelia

Radiolabeled HS was depolymerized by deaminative cleavage with low pH HNO_2. Disaccharides were isolated on a 1 × 120-cm Bio-Gel P-2 column. The resulting disaccharides were fractionated by SAX-HPLC as described in the text. The area under each peak in Fig. 3 was integrated to give the percentage composition in each sample. The numbers in the table are the average of three experiments which did not vary >5%.

Disaccharide	HS2	HS1
IdoA/GlcA-AMan$_R$	12.9	13.9
IdoA(2S)-AMan$_R$	53.4	44.8
GlcA-AMan$_R$(6S)	10.2	11.4
IdoA-AMan$_R$(6S)	3.4	2.7
IdoA(2S)-AMan$_R$(6S)	18.7	24.8
GlcA(2S)-AMan$_R$	1.0	1.8
GlcA-AMan$_R$(3S)	0.30	0.4
GlcA-AMan$_R$(3,6S)	0.15	0.2
Unknown	0.0	0.0

DISCUSSION

A mixture of structurally complex chain sequences are generated during the biosynthesis of HS and the data generated here represent the average for each pool of HS isolated. The analysis reported here makes clear that chain organization and fine structure differs systematically between key developmental stages, although the core protein carrying these different chains remains constant (6). By integrating all the structural data we have produced a simplified model to summarize the most significant changes in structure of the neuroepithelial HSs (Fig. 7). Previous studies characterizing skin fibroblast HS led to a model which posited the now widely accepted domain structure model of HS (11, 12). It was concluded that heparinase-sensitive disaccharides are located in short domains consisting of $GlcNSO_3$(±6S)-IdoA(±2S) repeats. These are separated by regions of polysaccharide that are heparinase resistant, enriched with *N*-acetylated disaccharides, and low in

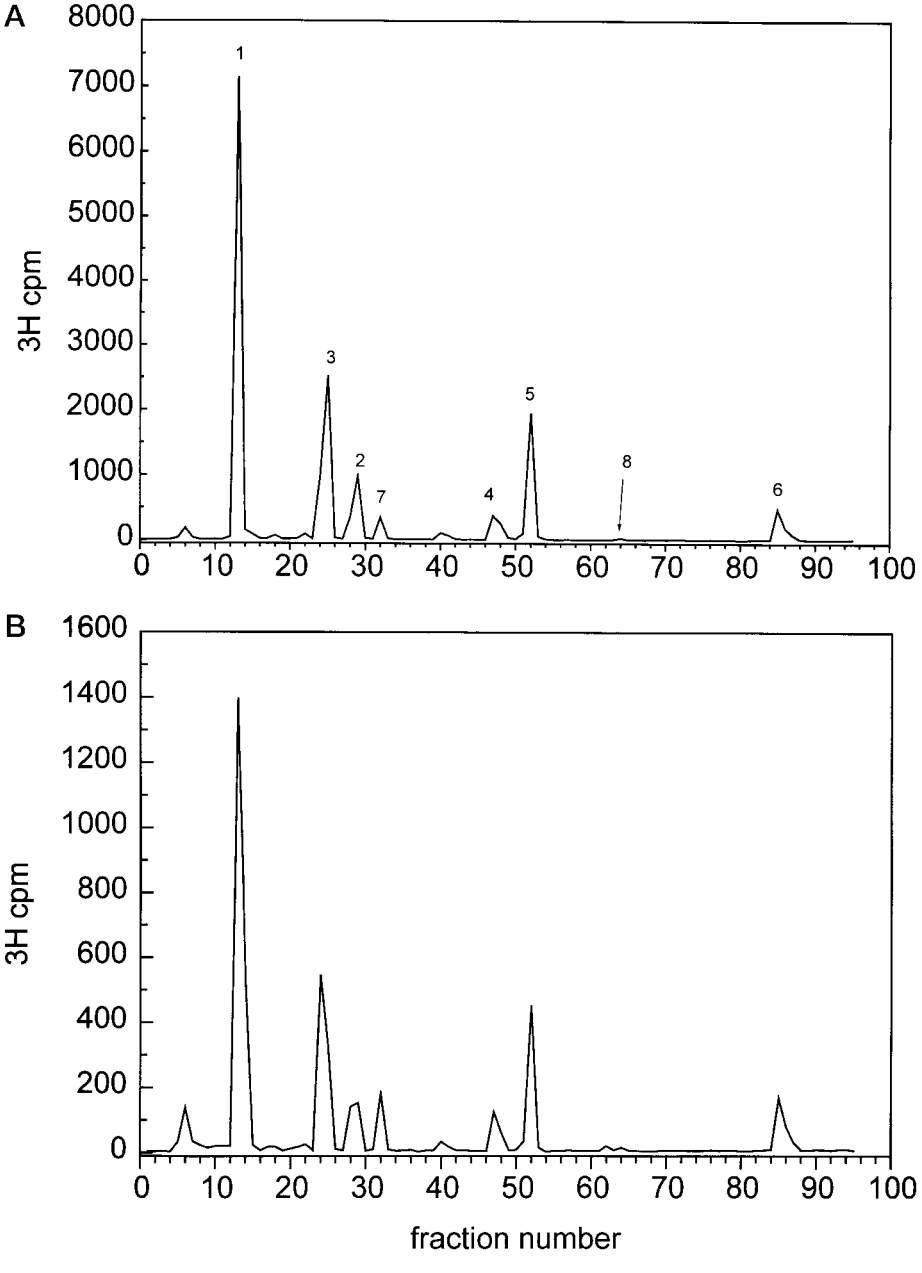

FIG. 4. **Strong anion exchange-high pressure liquid chromatography of HS disaccharides.** Disaccharides produced by lyase depolymerization were separated by SAX-HPLC. The elution times of the peaks were compared with whose of authentic standards and numerically labeled accordingly. The *numbers* correspond with numbers in Table IV which summarizes the relative abundance of each of the disaccharides. Representative elution profiles from HS2 disaccharides (*A*) and HS1 disaccharides (*B*).

TABLE IV
Lyase-derived disaccharide composition of heparan sulfate from the two sources of HS

Heparan sulfate was isolated and completely depolymerized with a mixture of heparan lyases. The resulting unsaturated disaccharides were isolated on a P-2 column and fractionated by strong anion exchange-HPLC. The area under each peak in Fig. 4 was integrated to calculate the percentage of each disaccharide in each sample. The numbers represent the average of three experiments which did not vary >5%. Over 97% disaccharides were recovered from each sample.

Peak	Disaccharide	HS2	HS1
		%	
1	ΔHexUA-GlcNAc	44.8	44.8
3	ΔHexUA-GlcNSO$_3$	21.5	20.0
2	ΔHexUA-GlcNAc(6S)	8.0	6.7
7	ΔHexUA(2S)-GlcNAc	2.4	4.3
4	ΔHexUA-GlcNSO$_3$(6S)	4.0	4.3
5	ΔHexUA(2S)-GlcNSO$_3$	12.4	11.3
8	ΔHexUA(2S)-GlcNAc(6S)	0.2	0.3
6	ΔHexUA(2S)-GlcNSO$_3$(6S)	4.1	6.4
9	Unknown	2.4	1.8

TABLE V
Sulfation characteristics of disaccharides from both HS pools

The calculations on sulfation characteristics shown are based on the overall disaccharide composition data (Table IV). The data indicate different levels of *O*-sulfation and sulfation ratios in these two HS samples.

Sulfation	HS2	HS1
	%	
Total sulfation/100 disaccharides	77.4	81
6-*O*-Sulfate	16.3	16.7
2-*O*-Sulfate	19.1	22.3
N-Sulfate	42.0	42.0
O-Sulfate	35.4	39
Ratios of sulfations		
2-*O*-Sulfate/6-*O*-sulfate	1.17	1.33
N-Sulfate/*O*-sulfate	1.19	1.08
N-Sulfate/2-*O*-sulfate	2.2	1.88
N-Sulfate/6-sulfate	2.58	2.51

both iduronic acid and sulfate moieties. Following this discovery, many other HS pools have been characterized which are similar in their overall organization (36, 37, 39, 40); this study demonstrates that HS derived from primary neuroepithelial cells conform to this structural theme, and to our knowledge represents the most detailed characterization to date of HS derived from primary cells. Apart from the increase in chain size and number of sulfated domains per chain in HS1, the data indicate basic similarities in domain structure, but with distinct *O*-sulfation patterns imposed on these domains. These alterations must be the basis for the changes in binding and activation of FGF2 and FGF1 previously reported (6). The main difference in fine structure between the two HSs is an obvious increase in sulfation at E12, which indicates that 2-*O*- and 6-*O*-sulfotransferases are significantly more active at the E12 as opposed to the E10 stage of development. However, it is when the disaccharides released by HNO_2 are studied that the distinctions become most clear, with HS1 showing a reproducibly higher amount of 6-*O*-S specifically in the disulfated species IdoA(2S)-AMan$_R$(6S); this shows that a highly regulated sulfotransferase activity is targeted to specific GlcNSO$_3$ residues within contiguous sequences of *N*-sulfated disaccharides. Data on the tetrasaccharides released by HNO_2 also support the view that regulation of *O*-sulfotransferases creates subtle differences in patterns of *O*-sulfation in the HS at different developmental stages.

Analysis of the disaccharides from HNO_2-degraded HS from the neuroepithelium corresponds with the relative amounts of HS-derived disaccharides found in the conditioned medium of a hepatocyte cell line, in that there is a high proportion of IdoA(2S)-AMan$_R$, followed by IdoA(2S)-AMan$_R$(6S) and IdoA/GlcA-AMan$_R$ (26). There is a significant decrease in IdoA(2S)-AMan$_R$ and an increase in GlcA-AMan$_R$(6S) in the transition from E10, the proliferative influence, to E12, the differentiative influence. In addition, HS1 is significantly different from HS2 in that it contains approximately 50% more of the trisulfated disaccharide HexA(2S)-GlcNSO$_3$(6S). Both of these results may reflect the crucial role suggested for 6-*O*-sulfates in binding FGF-1 and potentiating its activity *in vivo* (41, 42). Similar to hepatocytes, there is an increase in total sulfation in the E12 cells over less differentiated, E10 cells (26). Fedarko and Conrad (26) hypothesized that this reflects HS chains with longer sulfated domains and shorter non-sulfated domains in the confluent as opposed to dividing cells. In contrast, our data indicate that the two neuroepithelial HS species are very similar in domain sizes, with the main overall structural change in the E12-derived HS being the extra chain length, presence of a smaller proportion of *N*-acetylated sequences (which may contribute to the closer spacing of the heparinase cleavage sites) and a larger number of sulfated domains. Differences in the fine structure of HS recovered from syndecan-1 proteoglycan have been observed in terms of disaccharide composition, the arrangement of lyase cleavage sites, and in the length and number of highly sulfated domains. These changes appeared to underlie differences in the ability of HS to bind collagen but not FGF-2 (27, 40). This supports the idea proposed here that cells preferentially modify HS chains attached to a specific core protein to enable the HSPG to perform specific functions (43).

The filter binding assays suggest that HS2 has an enhanced affinity for FGF2 relative to HS1 and that this situation is reversed with respect to their binding of FGF1. While the differences may appear slight, HS1 and HS2 are, in fact pools of HS made in the developing tissue at the different ages. Consequently the subtle differences found here must reflect significant structural changes taking place in these pools during development which are necessary to appropriate function in an increasingly complex environment. These changes complement the expression of these two growth factors in the developing neuroepithelium (6, 7). It is also important to remember that this binding assay can assess one event only, the HS-FGF interaction, of the ternary interaction (HS-FGF-FGFR) thought to be required to initiate specific cell signaling. Thus, it is likely that distinct sequences required for biological activation of specific FGFs could be masked in simple binding assays by the presence of other inactive sequences which are nevertheless capable of binding FGFs. It is interesting to note that the intact HSPG binds growth factors with higher affinities than the heparan sulfate chains alone (6).[2]

One of the most interesting observations in this study is that the HS from undifferentiated, dividing cells is both smaller and simpler in structure than the HS from more differentiated, contact-inhibited cells. We have also undertaken studies on HS in an *in vitro* model with the 2.3D neuroepithelial cell line derived from E10 cells, in which the transition from growth to post-confluence parallels the E10 to E12 transition (6); overall, the differences between the samples of HS from less differentiated, growing cells and the HS from more mature, confluent cells follow similar trends to those observed in the primary cells (47). In view of the fact that the HS from the two less differentiated sources (E10 primary cells and growing 2.3D cells)

[2] V. Nurcombe, S. J. Joseph, and Y. Brickman, unpublished data.

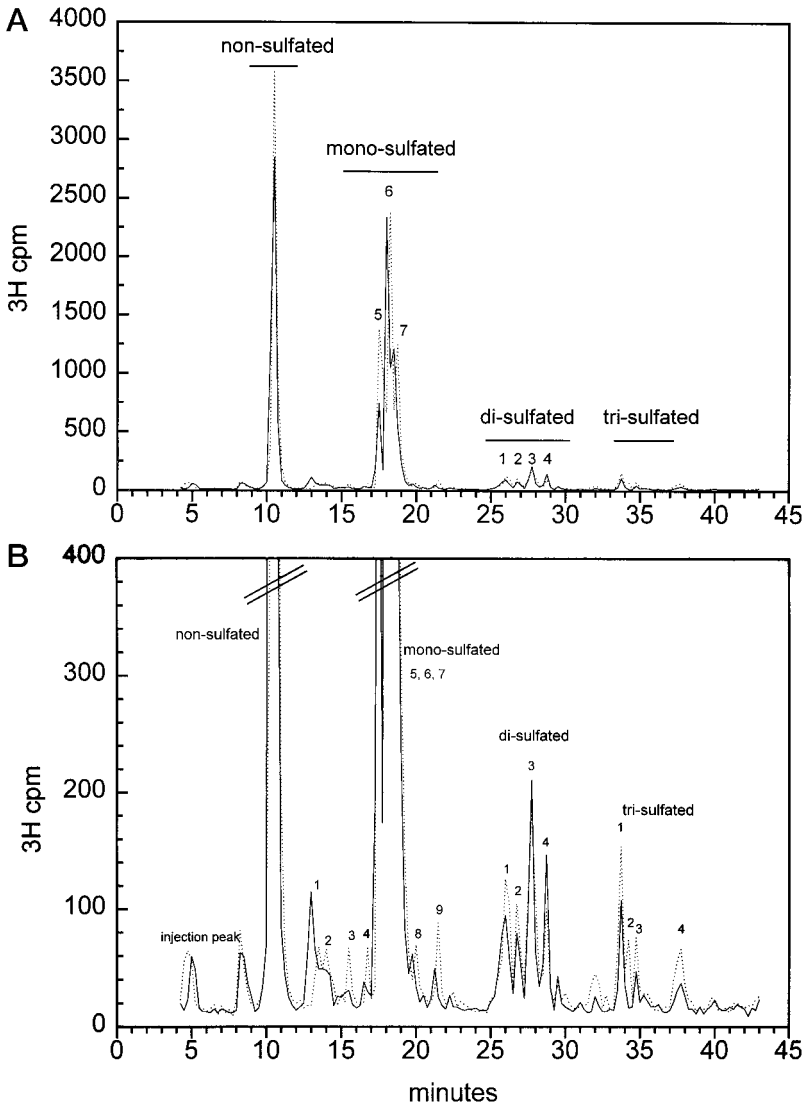

FIG. 5. **SAX-HPLC of the tetrasaccharides produced by HNO_2.** Tritiated tetrasaccharides produced by low pH HNO_2 were isolated from Bio-Gel P-2 low pressure chromatography, freeze dried, and separated by high pressure liquid chromatography and compared with dual $^{35}S/^{3}H$-labeled standard results. The *numbers* correspond to the order of the *left column* of Table IV. HS2 and HS1 profiles are presented in *A* with a complete profile, and *B*, an expanded axis highlighting the fractions which are low in abundance (HS2, —; HS1, ···).

bear the same FGF-2 potentiating activity (6), it follows that a particular HS sequence motif embedded within the sulfated domains may be common to both, and thus responsible for the formation of an FGF-2·FGFR ternary complex. A similar argument would hold for an FGF-1 activating subdomain within HS from E12 and confluent 2.3D cells. We know that HS from the growing 2.3D cell line contains a subdomain which promotes the interaction of FGF-2 with an FGFR (4). The exact composition of the sulfated domain which interacts with any specific FGF and its cognate FGF receptor remains to be determined; almost certainly the differences between chains that generate such significant differential specificity between ligands are quite subtle (18, 42, 43). However, the data presented here strongly suggest that regulation of patterns of 6-*O*-sulfation are a critical element. In addition, the spacing between the growth factor-binding and any receptor-binding regions of an HS molecule is likely to be significant to its recruitment into a ternary complex and thus its bioactivity (4, 44–46). Our results also carry the important implication that the use of heparin or heparin fragments in tissue culture experiments as analogues of HS to augment the activity of such agents as FGFs and other HS-binding proteins is likely to mask crucial and complex *in vivo* control mechanisms. Unlike HS, heparin does not consist of discrete sulfated domains; heparin is a more extensively epimerized and sulfated form of HS, with much larger proportions of disaccharides that are trisulfated.

TABLE VI
SAX-HPLC separation of the HS-derived tetrasaccharides produced by HNO_2

Tritiated tetrasaccharides derived by low pH HNO_2-treated heparan sulfates were originally separated by low pressure chromatography on a Bio-Gel P-2 column and were then further resolved by high pressure liquid chromatography. The percentage of each tetrasaccharide was determined by calculating the radioactivity in each peak and comparing it to the total radioactivity in all peaks combined. Tetrasaccharide peak numbers in the left column correspond to the peaks in Fig. 5. Minor peaks comprise less than 12% of total tetrasaccharides. The degree of sulfation was determined by comparison of these tritiated samples with peaks generated by dual $^{35}S/^{3}H$-radiolabeled samples (from Dr. Gordon Jayson, University of Manchester) run on the same column under identical conditions. The numbers represent the average of three separate experiments.

Sulfation number:peak	HS2	HS1
	%	
Non-sulfated	37.2	34.7
Monosulfated:1	1.5	0.6
Monosulfated:2	1.0	0.7
Monosulfated:3	0.3	0.2
Monosulfated:4	0.3	0.4
Monosulfated:5	7.7	17.3
Monosulfated:6	23.9	21.6
Monosulfated:7	18.4	13.1
Minor di- and trisulfated	9.7	11.4
Total	100	100

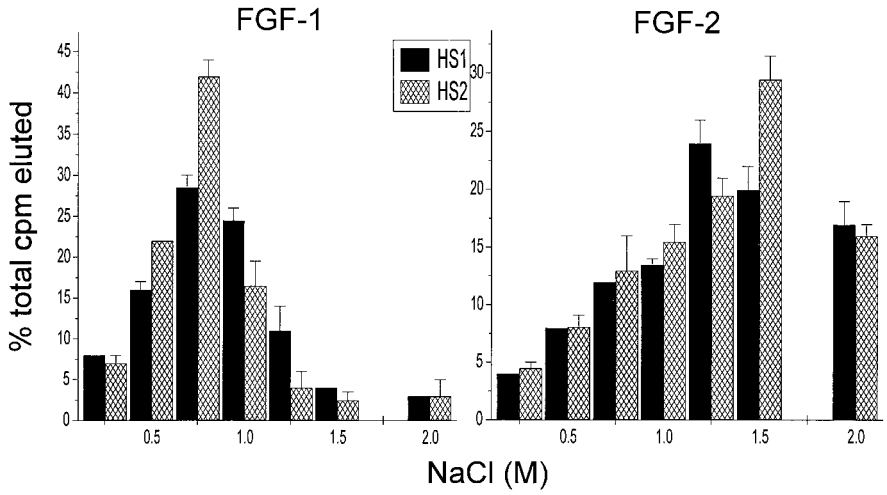

FIG. 6. **Filter binding assays for HS2 and HS1.** Filter binding assays were carried out as described under "Experimental Procedures" to assess the ability of HS1 and HS2 to interact with FGF-1 and FGF-2. ^{3}H-Labeled HS was incubated with the appropriate FGF and the complex immobilized on a nitrocellulose filter. The HS was then step eluted with increasing concentrations of NaCl shown. For the HS1 and HS2 assays the results represent the mean and standard errors for two independent experiments.

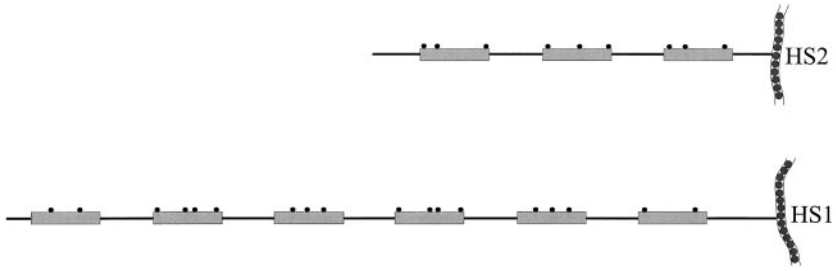

FIG. 7. **Hypothetical models of the heparan sulfate structures derived from the analysis of growing and differentiating neuroepithelial cells.** The model, based on the data presented here, proposes that HSs with altered structures are secreted by neuroepithelium to deal with changing expression patterns of extracellular FGFs. The most significant changes observed are increases in size, number of sulfated domains, and sulfation complexity (in particular the patterns of *O*-sulfation) as the cells mature. The *circles* denote the amino acids of the core protein, the *rectangular blocks* denote the sulfated domains, the *solid circles* denote 6-*O*-sulfate groups, and the *lines between* the *blocks* denote regions of *N*-acetylation.

As HS must serve a variety of different functions *in vivo*, the structural differences between HS chains must be designed to selectively produce specific functional properties. It is highly likely that these differences are the key to the individual and specific functions of HS in the extracellular environment, although methods for direct sequencing of HS saccharides will be required to substantiate this view. The fundamental hypothesis underlying the present study was that the functional changes in the FGF activating activities of secreted HS from either dividing or differentiating cells were due to systematic changes in the saccharide sequences of the HS chains. The differences in the structure of the two kinds of HS species found in this study are compatible with the idea that distinct HS sequences are expressed to selectively activate different FGFs, and that during embryonic development a non-committed cell type has the potential to vary the HS structure in response to epigenetic or environmental cues. Taken together with similar results from the structural analyses of other HS-binding molecules such as antithrombin III, hepatocyte growth factor, and interferon-γ, we predict that every molecule that requires HS for activation will have a distinct and specific disaccharide sequence motif dedicated to regulation of its biological activity. Thus, HS chains with different repertoires of distinct sequences will be generated by cells dependent on their need to orchestrate the activity of specific HS-binding proteins. Currently such molecules encompass members of the transforming growth factor-β family, the platelet-derived growth factor family, all of the FGFs, the pleiotropin-like family, and structural molecules such as the laminins, the fibronectins, the amyloid precursor protein family and the collagens, among many others. We further suggest that such HS-binding molecules will have configurations of basic amino acids which are spatially distinctive for the binding of such HS sequences.

Another important question raised by our data is how a single cell type regulates the switching of the production of one class of HS chain for another, closely related chain. We have as yet no data which informs us whether the sudden production of FGF-1 in E12 cells induces a change in HS synthesis, or whether the new HS is made in readiness for the growth factor switch. *In vivo*, this is an interesting question, as differentiation of hundreds of different subclasses of neurons and glia commences at these stages of mouse brain development. Recent evidence from our laboratory has tended to confirm our original hypothesis that the sudden synthesis of FGF-1 is a key event in the subsequent emergence of the neuronal lineage; if this is true, the change in HS specificity toward promotion of FGF-1 bioactivity becomes a seminal event in the appearance of neurons. This hypothesis can now be tested by specifically interfering with the enzymatic processes of those 6-*O*-sulfotransferases which construct the subtle differences in HS structure at each developmental stage, and monitoring for changes in subsequent rates of neuronal differentiation.

REFERENCES

1. Murphy, M., Drago, J., and Bartlett, P. F. (1990) *Neuroscience* **25,** 463–475
2. Rapraeger, A. C., Krufka, A., and Olwin, B. B. (1991) *Science* **252,** 1705–1708
3. Yayon, A., Klagsbrun, M., Esko, J. D., Leder, P., and Ornitz, D. M. (1991) *Cell* **64,** 841–848
4. Brickman, Y., Ford, M. D., Small, D. H., Bartlett, P. F., and Nurcombe, V. (1995) *J. Biol. Chem.* **270,** 24941–24948
5. Kan, M., Wang, F., Xu, J., Crabb, J. W., Hou, J., and McKeehan, W. L. (1993) *Science* **259,** 1918–1921
6. Nurcombe, V., Ford, M. D., Wildschut, J. A., and Bartlett, P. F. (1993) *Science* **260,** 103–106
7. Ford, M. D., Bartlett, P. F., and Nurcombe, V. (1994) *Neuroreport* **5,** 565–568
8. Gallagher, J. T., Lyon, M., and Steward, W. P. (1986) *Biochem. J.* **236,** 313–325
9. Lindahl, U. and Kjellen, L. (1987) in *The Biology of the Extracellular Matrix: Biology of Proteoglycans* (Wight, T. N., and Mecham, R. P., eds) pp. 59–104,

Harcourt Brace Jovanovich, Orlando, FL
10. Bienkowski, M. J., and Conrad, H. E. (1984) *J. Biol. Chem.* **259,** 12989–12996
11. Turnbull, J. E., and Gallagher, J. T. (1990) *Biochem. J.* **265,** 715–724
12. Turnbull, J. E., and Gallagher, J. T. (1991) *Biochem. J.* **273,** 553–559
13. Turnbull, J. E., and Gallagher, J. T. (1991) *Biochem. J.* **277,** 297–303
14. Gallagher, J. T., Turnbull, J. E., and Lyon, M. (1992) *Int. J. Biochem.* **24,** 553–560
15. Turnbull, J. E., and Gallagher, J. T. (1993) *Biochem. Soc. Trans.* **21,** 477–482
16. Saksela, O., Moscatelli, D., Sommer, A., and Rifkin, D. B. (1988) *J. Cell Biol.* **107,** 743–751
17. Turnbull, J. E., Fernig, D. G., Ke, Y., Wilkinson, M. C., and Gallagher, J. T. (1992) *J. Biol. Chem.* **267,** 10337–10341
18. Ishihara, M., Shaklee, P. N., Yang, Z., Liang, W., Stack, R. J., and Holme, K. (1994) *Glycobiology* **4,** 451–458
19. Zioncheck, T. F., Richardson, L., Liu, J., Chang, L., King, K. L., Bennett, G. L., Fugedi, P., Chamow, S. M., Schwall, R. H., and Stack, R. J. (1995) *J. Biol. Chem.* **270,** 16871–16878
20. Lyon, M., Deakin, J. A., Mizuno, K., Nakamura, T., and Gallagher, J. T. (1994) *J. Biol. Chem.* **269,** 11216–11223
21. Lortat-Jacob, H., Turnbull, J. E., and Grimaud, J. A. (1995) *Biochem. J.* **310,** 497–505
22. Bernard, O., Li, M., and Reid, H. H. (1991) *Proc. Natl. Acad. Sci. U. S. A.* **88,** 7625–7629
23. Winterbourne, D. J., and Mora, P. T. (1981) *J. Biol. Chem.* **256,** 4310–4320
24. Pejler, G., Backstrom, G., Lindahl, U., Paulsson, M., Dziadek, M., Fujiwara, S., and Timpl, R. (1987) *J. Biol. Chem.* **262,** 5036–5043
25. Pejler, G., and David, G. (1987) *Biochem. J.* **248,** 69–77
26. Fedarko, N. S., and Conrad, H. E. (1986) *J. Cell Biol.* **102,** 587–599
27. Kato, M., Wang, H., Bernfield, M., Gallagher, J. T., and Turnbull, J. E. (1994) *J. Biol. Chem.* **269,** 18881–18890
28. David, G., Bai, X. M., Van Der Schueren, B., Cassiman, J.-J., and Van den Berghe, H. (1992) *J. Cell Biol.* **119,** 961–975
29. Challacombe, J. F., and Elam, J. S. (1995) *Neurochem. Res.* **20,** 253–259
30. Wasteson, A. (1971) *J. Chromatography* **59,** 87–97
31. Shively, J. E., and Conrad, H. E. (1976) *Biochem.* **15,** 3932–3942
32. Bienkowski, M. J., and Conrad, H. E. (1985) *J. Biol. Chem.* **260,** 356–365
33. Linhardt, R., Turnbull, J., Wang, H., Loganathan, D., and Gallagher, J. (1991) *Biochemistry* **29,** 2611–2617
34. Maccarana, M., Casu, B., and Lindahl, U. (1993) *J. Biol. Chem.* **268,** 23898–23905
35. Turnbull, J. E. (1993) in *Methods in Molecular Biology* (Graham, J., and Higgins, J., eds) pp. 253–267, Humana Press Inc., Totowa, NJ
36. Hiscock, D. R. R., Canfield, A., and Gallagher, J. T. (1995) *Biochim. Biophys. Acta* **1244,** 104–112
37. Pye, D. A., and Kumar, S. (1995) *Biochim. Biophys. Acta* **1266,** 235–244
38. Gallagher, J. T., and Walker, A. (1985) *Biochem. J.* **230,** 665–674
39. Lyon, M., Deakin, J. A., and Gallagher, J. T. (1994) *J. Biol. Chem.* **269,** 11208–11215
40. Sanderson, R. D., Turnbull, J. E., Gallagher, J. T., and Lander, A. D. (1994) *J. Biol. Chem.* **269,** 13100–13106
41. Ishihara, M. (1994) *Glycobiology* **4,** 817–824
42. Guimond, S., Maccarana, M., Olwin, B., Lindahl, U., and Rapraeger, A. (1993) *J. Biol. Chem.* **268,** 23906–23914
43. Joseph, S. J., Ford, M. D., Barth, C., Portbury, S., Bartlett, P. F., Nurcombe, V., and Greferath, U. (1996) *Development* **122,** 3443–3452
44. Wang, F., Kan, M., Xu, J., Yan, G., and McKeehan, W. L. (1995) *J. Biol. Chem.* **270,** 10222–10230
45. Pantoliano, M. W., Horlick, R. A., Springer, B. A., Van Dyk, D. E., Tobery, T., Wetmore, D. R., Lear, J. D., Nahapetian, A. T., Bradley, J. D., and Sisk, W. P. (1994) *Biochemistry* **33,** 10229–10248
46. Kan, M., Wang, F., To, B., Gabriel, J. L., and McKeehan, W. L. (1996) *J. Biol. Chem.* **271,** 26143–26148
47. Brickman, Y. G., Nurcombe, V., Ford, M. D., Gallagher, J. T., Bartlett, P. F., and Turnbull, J. C. (1997) *Glycobiology* **7,** in press

Structural Modification of Fibroblast Growth Factor-binding Heparan Sulfate at a Determinative Stage of Neural Development

Yardenah G. Brickman, Miriam D. Ford, John T. Gallagher, Victor Nurcombe, Perry F. Bartlett and Jeremy E. Turnbull

J. Biol. Chem. 1998, 273:4350-4359.
doi: 10.1074/jbc.273.8.4350